

Quality of Performance Aware Data Transmission for Energy-Efficient Networked Control

TAKAHARU YAMANAKA¹, TAKANORI IWAI^{1,2}, AND RYOGO KUBO¹, (Member, IEEE)

¹Department of Electronics and Electrical Engineering, Keio University, Yokohama 223-8522, Japan

²System Platform Research Laboratories, NEC Corporation, Kawasaki 211-8666, Japan

Corresponding author: Takaharu Yamanaka (yamanaka.takaharu@kbl.elec.keio.ac.jp)

This work was supported by the JSPS KAKENHI under Grant 18K11275.

ABSTRACT The energy consumption of network interfaces in networked control systems (NCSs) must be reduced for sustainability. The sleep mechanisms of energy-efficient network interfaces for networked motor control systems, in which controller and motor devices are connected by communication networks, have attracted much interest in recent years. They reduce the energy consumption of network interfaces by making the transmitters installed on the controller and motor devices enter a sleep period when no data are to be transmitted. In a conventional send-on-delta (SoD)-based sleep control method, the network interfaces decide when to enter the sleep period based on the variations of the control input and response values. Although this method effectively reduces the communication rate for reducing energy consumption, it does not explicitly consider the quality of performance (QoP) or control performance such as tracking errors. In high-precision motion control systems, ensuring a certain QoP level is crucial. This study proposes a QoP-aware sleep control method for energy-efficient networked motor control systems to maintain the QoP at a certain level while operating the sleep mechanism. Here, the QoP is defined as the tracking error between the command and the response values. In the proposed method, network interfaces decide when to enter the sleep period based on the tracking error. Experimental results confirm that the QoP-aware sleep control method outperforms the SoD-based sleep control method in terms of the tracking errors (i.e., integral square error and steady-state error) at the expense of increased communication rates.

INDEX TERMS Data transmission, energy-efficient network, motion control, networked control system, remote control, quality of performance.


I. INTRODUCTION

Energy-efficient industrial development is strongly desired. However, recent industrial systems are incorporating information and communication technologies (ICTs) such as high-performance computing and networking that have increased energy consumption. In particular, the energy consumption of communication networks has increased continuously [1]–[3]. Therefore, the energy efficiency of networked systems has become an increasingly important issue, and as a result, various energy-efficient networking technologies have been developed and standardized.

Energy-Efficient Ethernet (EEE) is an energy-efficient communication protocol that uses a sleep mechanism to reduce energy consumption [4], [5]. EEE has been applied to

industrial Ethernet applications that require real-time communications [6], [7]. Energy-efficient passive optical networks (PONs) have been proposed for broadband optical access networks [8]–[10]. To reduce energy consumption in the optical network unit of a PON system, a cyclic sleep mechanism in which the network interface enters a sleep period when no data are to be transmitted is adopted. The sleep period can take a value of the order of tens of milliseconds, and the minimum sleep period is set in consideration of the wake-up time of optical transceivers [11]. A longer sleep period improves the energy efficiency at the expense of a longer latency. However, increased latency potentially has a negative impact on networked industrial systems.

A networked control system (NCS) is a type of networked industrial system [12], [13]. In particular, in a networked motor control system, controller and motor devices are connected by a communication network. In recent years, studies

The associate editor coordinating the review of this manuscript and approving it for publication was Guangcun Shan .

have investigated the energy efficiency of NCSs toward developing sustainable industrial systems. Event-triggered data transmission in network interfaces effectively reduces the amount of communication traffic and, in turn, reduces the energy consumption [14]. Send-on-delta (SoD) sampling is a sampling technique that is used to reduce the communication rate in a feedback control system over a network [15], [16]. SoD-based sampling methods utilize a threshold to determine whether to sample a signal. This threshold can be dynamically set depending on the network throughput to adapt to a time-varying network environment [17], [18]. SoD-based sampling methods have been applied to sensor signals [19] and control signals [20] in NCSs.

Funakoshi *et al.* [21] proposed an SoD-based sleep control method for sensor signals in a networked motor control system with optical network interfaces using the cyclic sleep mechanism. The network interfaces decide when to enter a sleep period based on the variation of response values, namely, sensor signals. The motor-side transmitter enters a sleep period when the difference between the latest and the previously transmitted response values is less than or equal to a threshold. However, both network-induced time delays and sleep-induced data losses degrade the control performance of such NCSs. To compensate for this performance degradation, a modified communication disturbance observer (MCDOB) was proposed [22]. SoD-based sleep control with the MCDOB could be applied to transmitters installed on both the controller and the motor sides, and it effectively reduced the communication rate and thereby realized energy savings. However, the conventional SoD-based sleep control method does not explicitly consider the control performance, such as tracking errors, and cannot maintain the control performance at a certain level.

Guaranteeing the control performance, that is, quality of performance (QoP), is an important requirement of industrial NCSs. Studies have already discussed the relationship between the quality of service (QoS) in network systems and the QoP in control systems [23], [24]. A low QoS may result in QoP degradation, such as tracking errors. Therefore, various approaches have been proposed to codesign control and communication systems [25]–[27]. Studies of NCSs have considered the relationship between energy and delay using codesign techniques [28], [29]. However, codesign techniques do not address the main issue in networked motor control systems, namely, the need to maintain the QoP at a certain level while making the network interfaces enter the sleep period as frequently as possible.

This study proposes a QoP-aware sleep control method that enables an energy-efficient networked motor control system to maintain the QoP at a certain level while operating the cyclic sleep mechanism. Here, the QoP is defined as the tracking error between the command and the response values in a feedback control system. The proposed method makes network interfaces (i.e., transmitters installed on the controller and motor sides) enter the sleep period if the tracking error is less than a threshold. Network-induced time delays

and sleep-induced data losses are compensated for by using the MCDOB, as with conventional SoD-based sleep control methods. Experimental results confirm that the QoP-aware sleep control method outperforms the SoD-based sleep control method in terms of tracking errors (i.e., integral square error (ISE) and steady-state error) at the expense of an increase in the communication rate. The proposed method is especially effective for NCSs with optical network interfaces that require sleep periods of the order of tens of milliseconds, such as NCSs over PONs [30]–[33].

The remainder of this article is organized as follows. Section II describes a networked motor control system with an energy-efficient network interface. Section III describes the conventional SoD-based sleep control method for energy-efficient NCSs. Section IV describes the proposed QoP-aware sleep control method that maintains the QoP at a certain level. Section V presents experimental results obtained using a direct current (DC) motor to compare the control performances of the conventional and the proposed methods. Finally, Section VI presents the conclusions of this study.

II. ENERGY-EFFICIENT NETWORKED CONTROL

This section first describes a networked motor control system. Then, an energy-efficient NCS configuration for enabling the sleep control of network interfaces is described. Finally, the MCDOB to compensate for network-induced time delays and sleep-induced data losses is described.

A. NETWORKED MOTOR CONTROL SYSTEM

This study considers a networked motor control system that can be applied to remote robot control and teleoperation systems. Figure 1 shows the block diagram of the NCS including a DC motor. This system is divided into the controller and the motor sides, both of which are connected by communication networks. The transmission delays for the forward and feedback paths are defined as T_1 and T_2 , respectively. These delays are considered constant values by introducing jitter buffers into the receivers to suppress delay variations [34].

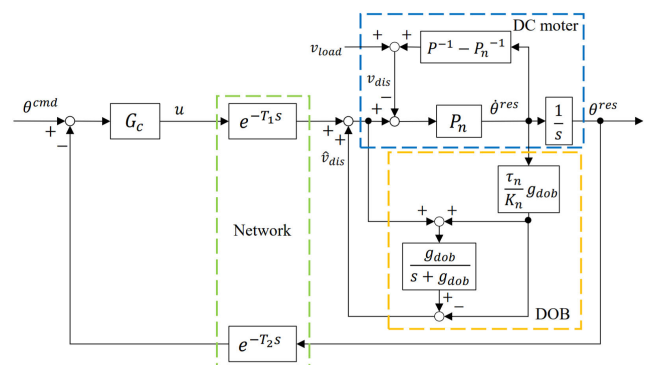


FIGURE 1. Angle control of a DC motor over networks.

The controller side includes a proportional-derivative (PD) controller G_c that is expressed as

$$G_c = \frac{\tau_n}{K_n}(K_p + K_d s), \quad (1)$$

where τ_n , K_n , K_p , K_d , and s denote the nominal time constant of the motor, nominal steady-state gain of the motor, proportional gain, derivative gain, and Laplace operator, respectively. The controller calculates the voltage reference u based on the angular command θ^{cmd} and the delayed signal of the angular response θ^{res} .

The motor side includes the DC motor and disturbance observer (DOB). The transfer function of the DC motor is expressed as

$$P = \frac{K}{\tau s + 1}. \quad (2)$$

Here, K and τ are the actual parameters of K_n and τ_n , respectively. Further, the nominal model of the DC motor P_n is expressed as (3)

$$P_n = \frac{K_n}{\tau_n s}. \quad (3)$$

The difference between P and P_n is treated as a system disturbance that includes an unpredictable load torque. This disturbance can be converted to v_{dis} in voltage as (4)

$$v_{dis} = v_{load} + (P^{-1} - P_n^{-1})\dot{\theta}^{res}, \quad (4)$$

where v_{load} and $\dot{\theta}^{res}$ denote a voltage disturbance caused by the load torque and the angular velocity response, respectively.

A DOB is implemented to reject the system disturbance [35], [36]. The DOB estimates the system disturbance \hat{v}_{dis} as

$$\hat{v}_{dis} = \frac{g_{dob}}{s + g_{dob}} v_{dis}, \quad (5)$$

where g_{dob} denotes the cut-off frequency of the DOB. The system disturbance can be equivalently estimated through the high-pass filter. A DOB with large cut-off frequency effectively rejects the system disturbance, resulting in robust motor control.

B. NCS WITH SLEEP-ENABLED TRANSCIEVERS

Figure 2 shows a configuration of the energy-efficient NCS with sleep-enabled transceivers. The ideal DC motor system completely compensated by the DOB, G_p , is represented as

$$G_p = \frac{P_n}{s}. \quad (6)$$

Figures 3(a) and 3(b) respectively show the operation of the sleep-enabled transceivers for the forward and feedback paths.

The operation for the forward path is as follows. The transmission delay is defined as $T_1 = k_{t1}t_c$, where k_{t1} and t_c denote the number of samples during T_1 and the control period, respectively. A data packet transmitted from the controller side arrives at the motor-side receiver after a lapse

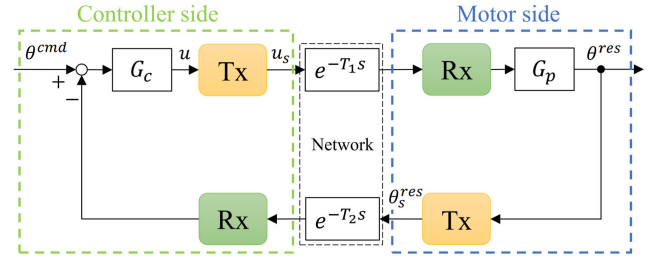


FIGURE 2. Energy-efficient NCS with sleep-enabled transceivers.

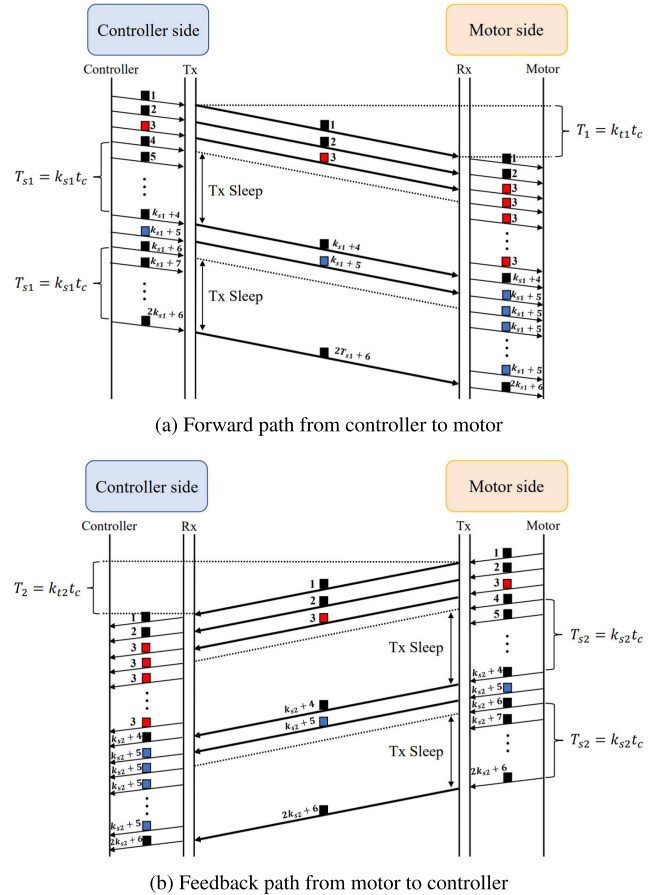


FIGURE 3. Operation of sleep-enabled transceivers.

of T_1 . When the transmitter is awake, the voltage reference u calculated by the controller is equal to the transmitted voltage reference u_s . By contrast, when the transmitter is asleep, the transmitter cannot transmit the voltage reference u . Therefore, the motor-side receiver uses the latest value received before entering the sleep period for $T_{s1} = k_{s1}t_c$, where k_{s1} denotes the number of samples during T_{s1} .

The operation for the feedback path is as follows. The transmission delay is defined as $T_2 = k_{t2}t_c$, where k_{t2} denotes the number of samples during T_2 . A data packet transmitted from the motor side arrives at the controller-side receiver after a lapse of T_2 . When the transmitter is awake, the angular response θ^{res} is equal to the transmitted angular

response θ_s^{res} . By contrast, when the transmitter is asleep, the transmitter cannot transmit the angular response θ^{res} . Therefore, the controller-side receiver uses the latest value received before entering the sleep period for $T_{s2} = k_{s2}t_c$, where k_{s2} denotes the number of samples during T_{s2} .

C. ANALYTICAL SYSTEM MODEL AND MCDOB

Figure 4 shows an analytical model of the energy-efficient NCS. The operations of sleep-enabled transceivers are modeled as the variable gains L_{s1} and L_{s2} . The gain L_{s1} varies based on the state variable S_c , which is the output of the forward sleep trigger (FWST) algorithm described in sections III and IV, as given by

$$L_{s1} = \begin{cases} \frac{u_s(k-1)}{u(k)} & \text{if } S_c = 0 \\ 1 & \text{if } S_c = 1 \end{cases}, \quad (7)$$

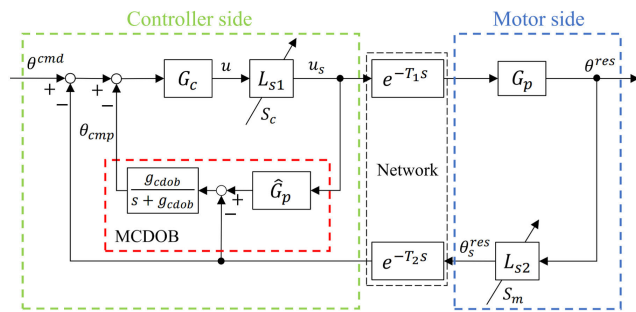


FIGURE 4. Time-delay and data-loss compensation by MCDOB.

where k denotes the sampling time. The state variable S_c takes a value of 0 if the transmitter is asleep and 1 if the transmitter is awake. The gain L_{s2} varies based on the state variable S_m , which is the output of the feedback sleep trigger (FBST) algorithm described in sections III and IV, as given by

$$L_{s2} = \begin{cases} \frac{\theta_s^{res}(k-1)}{\theta^{res}(k)} & \text{if } S_m = 0 \\ 1 & \text{if } S_m = 1 \end{cases}. \quad (8)$$

The state variable S_m takes a value of 0 if the transmitter is asleep and 1 if the transmitter is awake.

The transfer function from θ^{cmd} to θ^{res} when the MCDOB is not implemented, H_{nocmp} , is calculated as

$$H_{nocmp} = \frac{G_c G_p L_{s1} e^{-T_1 s}}{1 + G_c G_p L_{s1} L_{s2} e^{-(T_1 + T_2) s}}. \quad (9)$$

The denominator of H_{nocmp} includes the effects of network-induced time delays and sleep-induced data losses. To design a stable control system, all network delays and data losses must be considered.

The MCDOB compensates for network-induced time delays and sleep-induced data losses [22]. It estimates the effects of time delays and data losses on the system as a voltage disturbance, u_{dis} , given by

$$u_{dis} = (1 - L_{s2} e^{-(T_1 + T_2) s}) u_s. \quad (10)$$

The output of the MCDOB, θ_{cmp} , is given by

$$\theta_{cmp} = \frac{g_{cdob}}{s + g_{cdob}} (\hat{G}_p u_s - \theta^{res} L_{s2} e^{-T_2 s}), \quad (11)$$

where g_{cdob} and \hat{G}_p denote the cut-off frequency of the MCDOB and nominal motor model with the DOB, respectively. When $\hat{G}_p = G_p$ and $g_{cdob} \rightarrow \infty$, θ_{cmp} can be rewritten as

$$\theta_{cmp} = G_p u_{dis}. \quad (12)$$

Therefore, the transfer function from θ^{cmd} to θ^{res} when the MCDOB is implemented, H_{cmp} , is calculated as

$$H_{cmp} = \frac{G_c G_p L_{s1} e^{-T_1 s}}{1 + G_c G_p L_{s1}}. \quad (13)$$

The denominator of H_{cmp} does not include T_1 , T_2 , and L_{s2} , whereas that of H_{nocmp} includes them. When the MCDOB is implemented, the control system can be designed without considering the effects of network-induced time delays and sleep-induced data loss on the feedback path in terms of closed-loop stability. Because the denominator of H_{cmp} includes L_{s1} , the effect of the sleep-induced data loss on the forward path should be considered for the design of a stable control system. Sleep parameters such as the sleep period and thresholds are adjusted based on the effect of the sleep-induced data loss.

III. CONVENTIONAL SoD-BASED SLEEP CONTROL

This section describes the conventional SoD-based sleep control method with the MCDOB to reduce the communication rate.

A. SYSTEM CONFIGURATION

Figure 5 shows the configuration of the energy-efficient NCS with the SoD-based sleep control method. The delayed voltage reference and delayed angular response are defined as u_a and θ_a^{res} , respectively. The voltage reference calculated by the PD controller in every control period, u , and the latest voltage reference transmitted from the controller side, u_s , are input to the FWST. The FWST controls the state of the controller-side transmitter (i.e., asleep or awake) by using the state variable S_c . Further, the angular response measured by the sensor in every control period, θ^{res} , and the latest angular response transmitted from the motor side, θ_s^{res} , are input to the FBST. The FBST controls the state of the motor-side transmitter by using the state variable S_m .

B. SLEEP MECHANISM

Algorithm 1 shows the operation of the FWST for the SoD-based sleep control method. At the initial sampling time (i.e., $k = 0$), the state variable S_c is set to 1. If the transmitter is awake and the difference between the voltage reference $u(k)$ and the latest voltage reference transmitted $u_s(k-1)$ is less than the threshold h_1 , the transmitter enters a sleep period for $T_{s1} = k_{s1}t_c$ at sampling time k . After the sleep period lapses, the transmitter wakes up. This algorithm

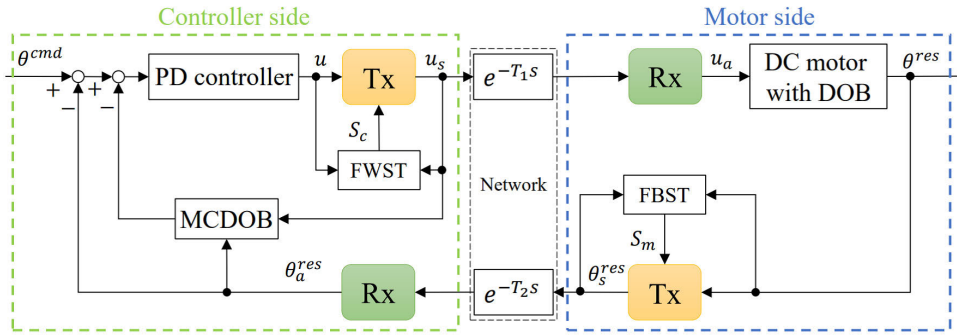


FIGURE 5. Energy-efficient NCS with the conventional SoD-based sleep control.

Algorithm 1 FWST in SoD-Based Sleep Control

```

 $S_c \leftarrow 1$ 
for  $k \leftarrow 0$  to  $k_{end}$  do
  if  $S_c = 1$  then
    if  $|u(k) - u_s(k-1)| < h_1$  then
       $k_0 \leftarrow k$ 
       $S_c \leftarrow 0$ 
    end if
  else if  $k \geq k_0 + k_{s1}$  then
     $S_c \leftarrow 1$ 
  end if
end for

```

Algorithm 2 FBST in SoD-Based Sleep Control

```

 $S_m \leftarrow 1$ 
for  $k \leftarrow 0$  to  $k_{end}$  do
  if  $S_m = 1$  then
    if  $|\theta^{res}(k) - \theta_s^{res}(k-1)| < h_2$  then
       $k_0 \leftarrow k$ 
       $S_m \leftarrow 0$ 
    end if
  else if  $k \geq k_0 + k_{s2}$  then
     $S_m \leftarrow 1$ 
  end if
end for

```

is executed in every control period until the ending sampling time k_{end} . The motor-side receiver keeps utilizing the latest voltage reference received as $u_a(k) = u_s(k - k_{t1})$ when not receiving a new voltage reference at sampling time k .

Algorithm 2 shows the operation of the FBST for the SoD-based sleep control method. At the initial sampling time (i.e., $k = 0$), the state variable S_m is set to 1. If the transmitter is awake and the difference between the angular response $\theta^{res}(k)$ and the latest angular response transmitted $\theta_s^{res}(k - 1)$ is less than the threshold h_2 , the transmitter enters the sleep period for $T_{s2} = k_{s2}t_c$ at sampling time k . After the sleep period lapses, the transmitter wakes up. This algorithm is executed in every control period until the ending sampling time k_{end} . The controller-side receiver keeps utilizing the latest angular response received as $\theta_a^{res}(k) = \theta_s^{res}(k - k_{t2})$ when not receiving a new angular response at sampling time k .

IV. PROPOSED QoP-AWARE SLEEP CONTROL

This section describes the proposed QoP-aware sleep control method with the MCDOB to maintain the QoP at a certain level while operating the sleep mechanism.

A. SYSTEM CONFIGURATION

Figure 6 shows the configuration of the energy-efficient NCS with the QoP-aware sleep control method. The error signal between the angular command θ^{cmd} and the delayed angular response θ_a^{res} , e , is input to the FWST. The FWST controls

the state of the controller-side transmitter by using the state variable S_c . In addition, the angular command θ^{cmd} is transmitted to the motor side when the transmitter is awake. The latest angular command transmitted from the controller side is defined as θ_s^{cmd} . Further, the angular response measured by the sensor in every control period, θ^{res} , and the delayed angular command, θ_a^{cmd} , are input to the FBST. The FBST controls the state of the motor-side transmitter by using the state variable S_m .

B. SLEEP MECHANISM

Algorithm 3 shows the operation of the FWST for the QoS-aware sleep control method. At the initial sampling time (i.e., $k = 0$), the state variable S_c is set to 1. If the transmitter is awake and the absolute error between the angular command $\theta^{cmd}(k)$ and the delayed angular response $\theta_s^{res}(k - 1)$, $|e(k)|$, is less than the threshold h_e , the transmitter enters the sleep period for $T_{s1} = k_{s1}t_c$ at sampling time k . After the sleep period lapses, the transmitter wakes up. This algorithm is executed in every control period until the ending sampling time k_{end} . The motor-side receiver keeps utilizing the latest voltage reference received as $u_a(k) = u_s(k - k_{t1})$ when not receiving a new voltage reference at sampling time k .

Algorithm 4 shows the operation of the FBST for the QoP-aware sleep control method. At the initial sampling time (i.e., $k = 0$), the state variable S_m is set to 1. If the transmitter is awake and the difference between the

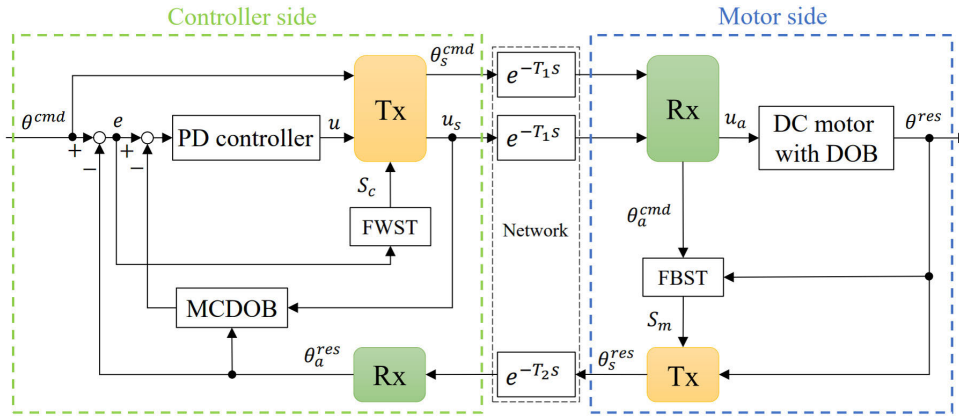


FIGURE 6. Energy-efficient NCS with proposed QoP-aware sleep control.

Algorithm 3 FWST in QoP-Aware Sleep Control

```

Sc ← 1
for k ← 0 to kend do
  if Sc = 1 then
    if |e(k)| < he then
      k0 ← k
      Sc ← 0
    end if
  else if k ≥ k0 + ks1 then
    Sc ← 1
  end if
end for
    
```

angular response $\theta^{res}(k)$ and the delayed angular command $\theta_a^{cmd}(k) = \theta_s^{cmd}(k - k_{t1})$ is less than the threshold h_e , the transmitter enters the sleep period for $T_{s2} = k_{s2}t_c$ at the next sampling time $k + 1$ after transmitting $\theta^{res}(k)$ as $\theta_s^{res}(k)$ to the controller side at sampling time k . The transmitter enters the sleep period at the next sampling time because the FWST cannot recognize the latest angular response that satisfies the sleep condition if the transmitter enters the sleep period at sampling time k . After the sleep period lapses, the transmitter wakes up. This algorithm is executed in every control period until the ending sampling time k_{end} . The controller-side receiver keeps utilizing the latest angular response received as $\theta_a^{res}(k) = \theta_s^{res}(k - k_{t2})$ when not receiving a new angular response at sampling time k .

V. EXPERIMENT

This section describes the experimental setup of the motion control system and presents the results of the experiments performed to confirm the effectiveness of the proposed QoP-aware sleep control method.

A. SETUP

Experiments were performed using a networked motion control system to compare the control performances of the conventional SoD-based and proposed QoP-aware sleep control

Algorithm 4 FBST in QoP-Aware Sleep Control

```

Sm ← 1
sleep_flag ← 1
for k ← 0 to kend do
  if Sm = 1 then
    if sleep_flag = 1 then
      if |θres(k) - θacmd(k)| < he then
        sleep_flag ← 0
      end if
    else
      k0 ← k
      Sm ← 0
    end if
  else if k ≥ k0 + ks2 then
    Sm ← 1
    sleep_flag ← 1
  end if
end for
    
```

methods, hereafter referred to as simply the SoD-based and QoP-aware methods, respectively. Figure 7 shows the experimental system including a controller device and a DC motor. The PD controller, MCDOB, DOB, and sleep control methods were implemented in the controller device in a LabVIEW environment. The transmission delays and transceiver operations were emulated in the same environment. The controller device and DC motor were connected via a voltage-controlled power amplifier to drive the motor. The rotational angle of the motor was measured by an encoder.

Table 1 shows the control parameters set in the experiments. We designed the proportional gain K_p and derivative gain K_d so as to meet the critical damping condition. In the SoD-based method, the voltage threshold h_1 and angular threshold h_2 were experimentally determined by considering the system stability. In the QoP-aware method, the error threshold h_e can be determined based on the control performance an application requires. In this study, the threshold was set to 0.02 rad.

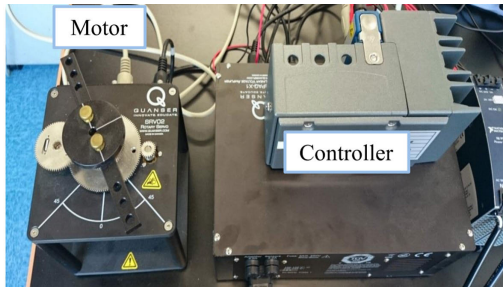


FIGURE 7. Experimental system.

TABLE 1. Control Parameters Set in the Experiments

Proportional gain of PD controller	K_p	225
Derivative gain of PD controller	K_d	30
Nominal steady-state gain of motor	K_n	1.53
Nominal time constant of motor	τ_n	0.0254
Cut-off frequency of DOB	g_{dob}	200 rad/s
Cut-off frequency of MCDOB	g_{cdob}	200 rad/s
Transmission delay for forward path	T_1	20 ms
Transmission delay for feedback path	T_2	20 ms
Voltage threshold for SoD-based method	h_1	0.01 V
Angular threshold for SoD-based method	h_2	0.01 rad
Error threshold for QoP-aware method	h_e	0.02 rad
Control period	t_c	0.001 s

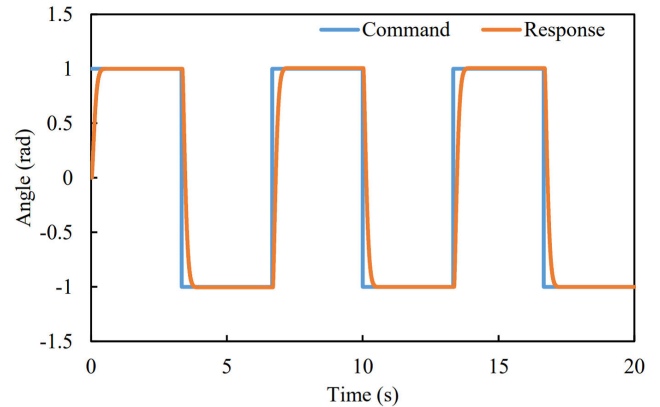
In the experiments, a square wave was input as an angular command for 20 s. The amplitude and frequency of the square wave were set to 1 rad and 0.15 Hz, respectively. The control performances of the SoD-based and QoP-aware methods were compared in terms of the communication rate, ISE, and steady-state error when the sleep periods T_{s1} and T_{s2} varied. The communication rate is defined as the time occupancy of the period during which a transmitter is awake. A lower communication rate indicates lower energy consumption in the transmitter. The ISE is defined as

$$\sum_{k=0}^{k_{end}} \left(\theta^{cmd}(k) - \theta^{res}(k) \right)^2 t_c. \quad (14)$$

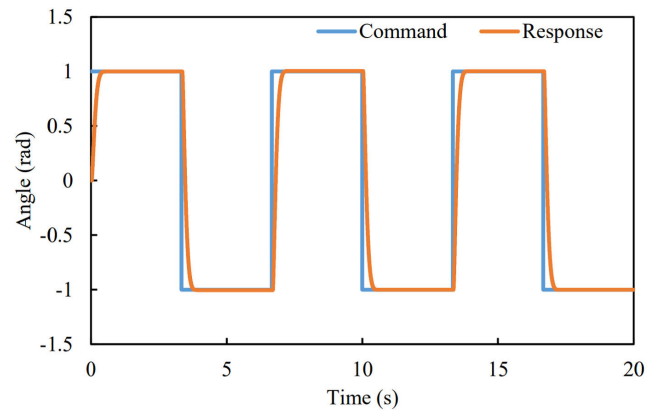
The steady-state error is defined as the average absolute error between the angular command and the converged value of the angular response for each step input. In the experiments, the square wave input for 20 s was divided into six step inputs. The steady-state error was calculated based on the converged value of each step response.

B. RESULTS

Figures 8, 9, and 10 show the angular responses for $T_{s1} = T_{s2} = 10$ ms, 60 ms, and 80 ms, respectively. Each figure shows the results obtained using the SoD-based and QoP-aware methods. The minimum sleep periods were set to 10 ms because the wake-up time of an optical transceiver was assumed to be of the order of milliseconds [11]. Moreover, the maximum sleep periods were set to 80 ms because a persistent oscillation was generated when the sleep periods were set to 90 ms. In Fig. 8, the angular responses converged



(a) SoD-based method

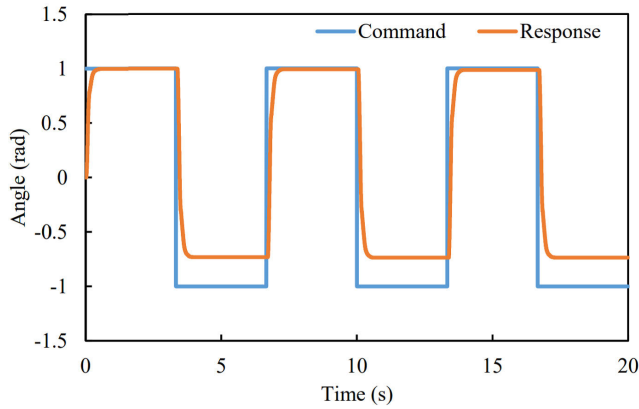


(b) QoP-aware method

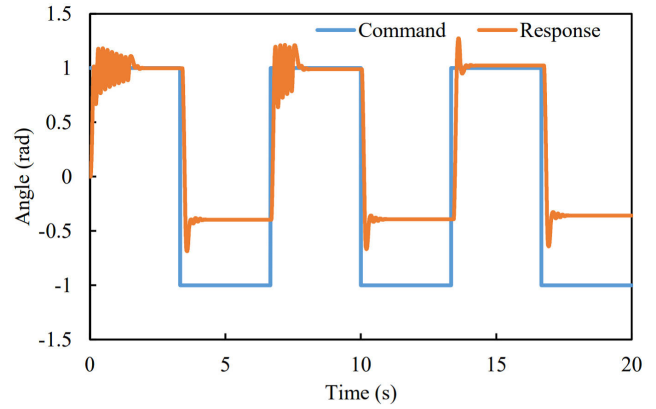
FIGURE 8. Angular responses ($T_{s1} = T_{s2} = 10$ ms).

without any oscillations for both the SoD-based and the QoP-aware methods. In Figs. 9 and 10, the angular responses of the SoD-based method generated larger errors than those of the QoP-aware methods. This is because the SoD-based method evaluated not the errors but the variations of the data to be transmitted, whereas the QoP-aware method determined the sleep timing based on the errors. The asymmetric response characteristics of the SoD-based method for positive and negative values can be attributed to the disturbance exerted on the motor.

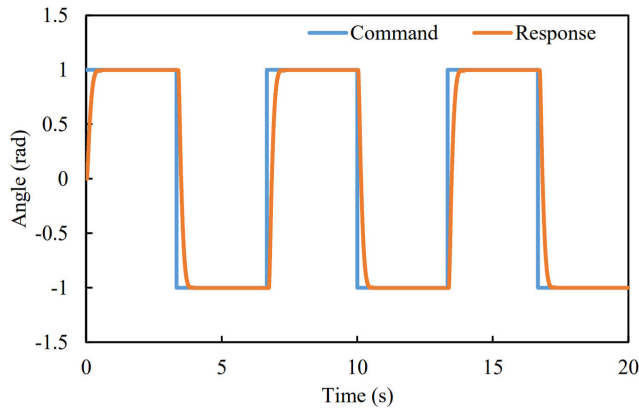
Figure 11 shows the communication rates when the sleep periods varied from 10 to 80 ms. The sleep periods T_{s1} and T_{s2} were set to the same value. The communication rates of the controller-side transmitter for the forward path and the motor-side transmitter for the feedback path are shown separately. The QoP-aware method generated larger communication rates than the SoD-based method for all sleep periods. This is because it operated based on the error, and the transmitters rarely entered the sleep period in transient states. Both the SoD-based and the QoP-aware methods tended to decrease the communication rate when the sleep period increased. In particular, the SoD-based method increased the communication rate for a sleep period longer than 70 ms because the transient responses had some oscillation.



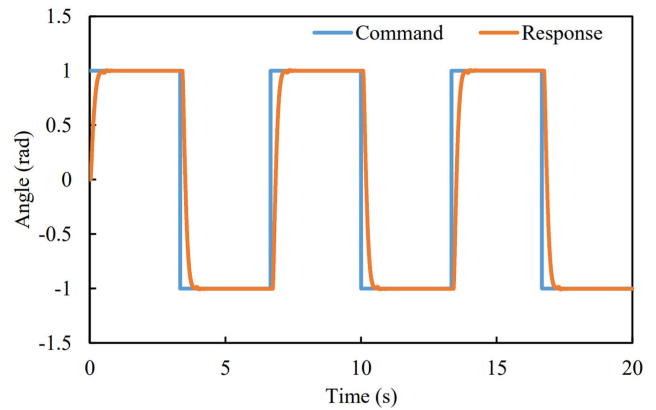
(a) SoD-based method



(a) SoD-based method



(b) QoP-aware method



(b) QoP-aware method

FIGURE 9. Angular responses ($T_{s1} = T_{s2} = 60$ ms).

tions, as shown in Fig. 10(a). The oscillations induced the loss of the sleep timing, resulting in an increased communication rate despite the long sleep period.

Figure 12 shows the ISEs when the sleep periods varied from 10 to 80 ms. The sleep periods T_{s1} and T_{s2} were set to the same value. Both the SoD-based and the QoP-aware methods tended to increase the ISE when the sleep period increased because a large sleep period resulted in the loss of the data to be transmitted. In particular, the ISEs of the SoD-based method were approximately 1.3 times and 1.8 times larger than those of the QoP-aware method when the sleep periods were 70 ms and 80 ms, respectively. This is because the oscillations of the angular response in the SoD-based method increased the period of transient states, as shown in Fig. 10(a), and increased the errors in the transient states.

Figure 13 shows the steady-state errors when the sleep periods varied from 10 to 80 ms. The sleep periods T_{s1} and T_{s2} were set to the same value. The QoP-aware method kept the steady-state error less than 0.005 rad regardless of the sleep period because it controls the sleep timing based on the error between the angular command and the angular response even when the angular response is in the steady state. By contrast, the SoD-based method generated a larger steady-state error than the QoP-aware method for all sleep

FIGURE 10. Angular responses ($T_{s1} = T_{s2} = 80$ ms).

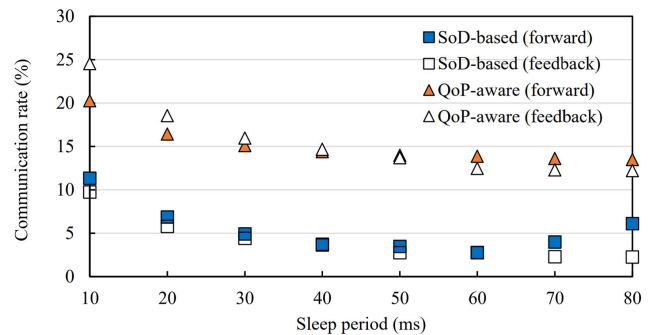


FIGURE 11. Communication rate for each sleep period ($T_{s1} = T_{s2}$).

periods and tended to increase the steady-state error when the sleep period increased. This is because it did not consider the error and only considered the variations of the data to be transmitted.

The above results indicate that the QoP-aware method could maintain the tracking errors, namely, the ISE and the steady-state error, at a constant level at the expense of an increased communication rate compared to that in the SoD-based method regardless of the sleep period. When small sleep periods such as 10 ms are applied to the transmitter, the superior tracking errors of the QoP-aware method

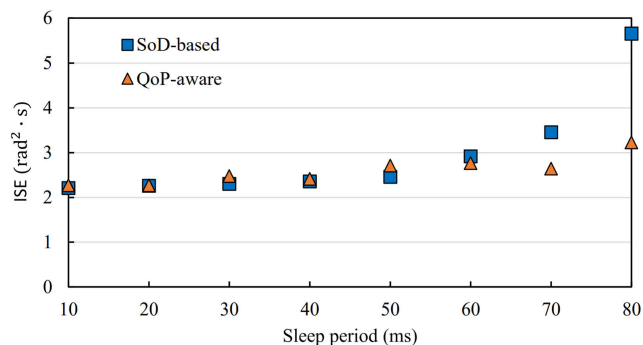


FIGURE 12. ISE for each sleep period ($T_{s1} = T_{s2}$).

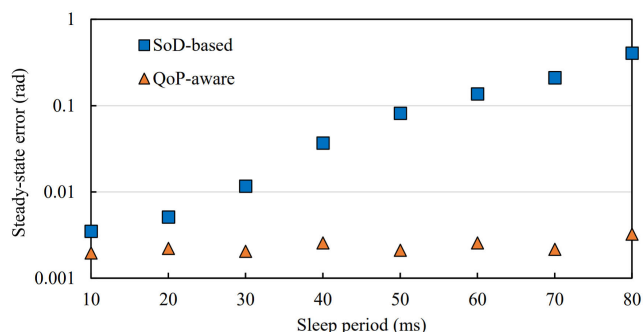


FIGURE 13. Steady-state error for each sleep period ($T_{s1} = T_{s2}$).

cannot be confirmed because the communication rate is comparatively high. However, a configurable range of the sleep period depends on the wake-up time of the transmitter, and a larger sleep period effectively decreases the energy consumption of transmitter circuits. Therefore, the advantage of the QoP-aware method lies in maintaining the tracking errors at a constant level even if the sleep period increases.

VI. CONCLUSION

This study proposed a QoP-aware sleep control method for network interfaces for energy-efficient networked motor control systems. The conventional SoD-based sleep control method could not guarantee tracking errors (i.e., ISE and steady-state error) because it determined the sleep timing based on the variations of data to be transmitted. By contrast, the proposed QoP-aware sleep control method maintained the tracking errors at a constant level by determining the sleep timing based on the error between the angular command and the angular response. Experimental results confirmed that the QoP-aware method maintained the tracking errors at a constant level at the expense of an increased communication rate compared to that in the SoD-based method regardless of the sleep period.

The proposed QoP-aware sleep control method can be applied to network interfaces with large sleep periods of the order of tens of milliseconds. Although this study applies the proposed QoP-aware sleep control method to a networked motion control system, this method can be utilized in any

NCSs by setting the threshold to an application-oriented value. Future studies will aim to consider various QoP requirements other than tracking errors and various network environments such as unreliable wireless networks with large time-varying delays. To evaluate the QoP in an integrated manner, a novel index combining multiple performance metrics will be needed.

REFERENCES

- [1] Y. Zhang, P. Chowdhury, M. Tornatore, and B. Mukherjee, "Energy efficiency in telecom optical networks," *IEEE Commun. Surveys Tuts.*, vol. 12, no. 4, pp. 441–458, 2010.
- [2] S. Lambert, W. Van Heddeghem, W. Vereecken, B. Lannoo, D. Colle, and M. Pickavet, "Worldwide electricity consumption of communication networks," *Opt. Exp.*, vol. 20, no. 26, p. B513, Dec. 2012.
- [3] P. Gandotra, R. K. Jha, and S. Jain, "Green communication in next generation cellular networks: A survey," *IEEE Access*, vol. 5, pp. 11727–11758, 2017.
- [4] K. Christensen, P. Reviriego, B. Nordman, M. Bennett, M. Mostowfi, and J. Maestro, "IEEE 802.3az: The road to energy efficient Ethernet," *IEEE Commun. Mag.*, vol. 48, no. 11, pp. 50–56, Nov. 2010.
- [5] X. Pan, T. Ye, and T. T. Lee, "Power efficiency and delay trade-off of 100G energy efficient Ethernet protocol," *IEEE Access*, vol. 8, pp. 106746–106764, 2020.
- [6] J. A. Maestro and P. Reviriego, "Energy efficiency in industrial Ethernet: The case of powerlink," *IEEE Trans. Ind. Electron.*, vol. 57, no. 8, pp. 2896–2903, Aug. 2010.
- [7] F. Tramarin and S. Vitturi, "Strategies and services for energy efficiency in real-time Ethernet networks," *IEEE Trans. Ind. Informat.*, vol. 11, no. 3, pp. 841–852, Jun. 2015.
- [8] R. Kubo, J.-I. Kani, Y. Fujimoto, N. Yoshimoto, and K. Kumozaki, "Adaptive power saving mechanism for 10 gigabit class PON systems," *IEICE Trans. Commun.*, vol. E93-B, no. 2, pp. 280–288, Feb. 2010.
- [9] Y. Maneyama and R. Kubo, "QoS-aware cyclic sleep control with proportional-derivative controllers for energy-efficient PON systems," *IEEE/OSA J. Opt. Commun. Netw.*, vol. 6, no. 11, pp. 1048–1058, Nov. 2014.
- [10] M. Zhu, X. Zeng, Y. Lin, and X. Sun, "Modeling and analysis of watchful sleep mode with different sleep period variation patterns in PON power management," *IEEE/OSA J. Opt. Commun. Netw.*, vol. 9, no. 9, pp. 803–812, Sep. 2017.
- [11] J. Mandin. (Sep. 2008). EPON power saving via sleep mode. IEEE P802.3av Task Force Meeting. [Online]. Available: http://www.ieee802.org/3/av/public/2008_09/index.html
- [12] X.-M. Zhang, Q.-L. Han, and X. Yu, "Survey on recent advances in networked control systems," *IEEE Trans. Ind. Informat.*, vol. 12, no. 5, pp. 1740–1752, Oct. 2016.
- [13] Y. Zhan, Y. Xia, and A. V. Vasilakos, "Future directions of networked control systems: A combination of cloud control and fog control approach," *Comput. Netw.*, vol. 161, pp. 235–248, Oct. 2019.
- [14] M. Miskowicz, "Event-based sampling strategies in networked control systems," in *Proc. 10th IEEE Workshop Factory Commun. Syst. (WFCS)*, May 2014, pp. 1–10.
- [15] V. Vasyutynskyy and K. Kabitzsch, "A comparative study of PID control algorithms adapted to send-on-delta sampling," in *Proc. IEEE Int. Symp. Ind. Electron.*, Jul. 2010, pp. 3373–3379.
- [16] J. A. Romero, R. Sanchis, and E. Arrebola, "Experimental study of event based PID controllers with different sampling strategies. Application to brushless DC motor networked control system," in *Proc. 25th Int. Conf. Inf., Commun. Autom. Technol. (ICAT)*, Oct. 2015, pp. 1–6.
- [17] M. Diaz-Cacho, E. Delgado, P. Falcon, and A. Barreiro, "Threshold selection algorithm for basic send-on-delta sampling strategies," in *Proc. 42nd Annu. Conf. IEEE Ind. Electron. Soc. (IECON)*, Oct. 2016, pp. 359–364.
- [18] M. Diaz-Cacho, P. Falcon, E. Delgado, and J. Lopez, "Send-on-delta strategy for networked-control-systems based on network status," in *Proc. 5th Int. Conf. Event-Based Control, Commun., Signal Process. (EBCCSP)*, May 2019, pp. 1–6.
- [19] J. Ploennigs, V. Vasyutynskyy, and K. Kabitzsch, "Comparative study of energy-efficient sampling approaches for wireless control networks," *IEEE Trans. Ind. Informat.*, vol. 6, no. 3, pp. 416–424, Aug. 2010.

- [20] C. Peng, D. Yue, and M.-R. Fei, "A higher energy-efficient sampling scheme for networked control systems over IEEE 802.15.4 wireless networks," *IEEE Trans. Ind. Informat.*, vol. 12, no. 5, pp. 1766–1774, Oct. 2016.
- [21] T. Funakoshi and R. Kubo, "Cyclic sleep control of network interfaces in feedback path for energy-efficient networked control systems," in *Proc. 2nd IEEJ Int. Workshop Sens., Actuation, Motion Control, Optim. (SAMCON)*, Mar. 2016, paper V-6.
- [22] T. Yamanaka, K. Yamada, R. Hotchi, and R. Kubo, "Simultaneous time-delay and data-loss compensation for networked control systems with energy-efficient network interfaces," *IEEE Access*, vol. 8, pp. 110082–110092, 2020.
- [23] S. Soucek and T. Sauter, "Quality of service concerns in IP-based control systems," *IEEE Trans. Ind. Electron.*, vol. 51, no. 6, pp. 1249–1258, Dec. 2004.
- [24] S. R. M. Canovas and C. E. Cagnasca, "Implementation of a control loop experiment in a network-based control system with LonWorks technology and IP networks," *IEEE Trans. Ind. Electron.*, vol. 57, no. 11, pp. 3857–3867, Nov. 2010.
- [25] P. Marti, J. Yopez, M. Velasco, R. Villa, and J. M. Fuertes, "Managing quality-of-control in network-based control systems by controller and message scheduling co-design," *IEEE Trans. Ind. Electron.*, vol. 51, no. 6, pp. 1159–1167, Dec. 2004.
- [26] X. Wang and N. Hovakimyan, "Distributed control of uncertain networked systems: A decoupled design," *IEEE Trans. Autom. Control*, vol. 58, no. 10, pp. 2536–2549, Oct. 2013.
- [27] L. Lyu, C. Chen, C. Hua, S. Zhu, and X. Guan, "Co-design of stabilisation and transmission scheduling for wireless control systems," *IET Control Theory Appl.*, vol. 11, no. 11, pp. 1767–1778, Jul. 2017.
- [28] Y. Maneyama, M. Tadokoro, D. Murayama, M. Yoshino, K.-I. Suzuki, and R. Kubo, "Sleep period randomization for networked control systems over energy-efficient EPONs," *IEICE Commun. Exp.*, vol. 4, no. 4, pp. 130–135, 2015.
- [29] Y. Sadi and S. Coleri Ergen, "Energy and delay constrained maximum adaptive schedule for wireless networked control systems," *IEEE Trans. Wireless Commun.*, vol. 14, no. 7, pp. 3738–3751, Jul. 2015.
- [30] R. Imai and R. Kubo, "Cloud-based remote motion control over FTTH networks for home robotics," in *Proc. IEEE 3rd Global Conf. Consum. Electron. (GCCE)*, Oct. 2014, pp. 565–566.
- [31] E. Wong, M. Pubudini Imali Dias, and L. Ruan, "Predictive resource allocation for tactile Internet capable passive optical LANs," *J. Lightw. Technol.*, vol. 35, no. 13, pp. 2629–2641, Jul. 1, 2017.
- [32] M. Maier, A. Ebrahimzadeh, and M. Chowdhury, "The tactile Internet: Automation or augmentation of the human?" *IEEE Access*, vol. 6, pp. 41607–41618, 2018.
- [33] R. Kubo, T. Michigami, K. Yamada, and M. Yoshino, "Demonstration of wide-area networked motion control over long-reach 10G-EPON based on optical access edge computing," in *Proc. 24th OptoElectronics Commun. Conf. (OECC) Int. Conf. Photon. Switching Comput. (PSC)*, Jul. 2019, paper TuA3-5.
- [34] A. Kato, H. Nishi, and K. Ohnishi, "Network bilateral control system with jitter buffer," *IEEJ Trans. Ind. Appl.*, vol. 126, no. 12, pp. 1737–1738, 2006.
- [35] K. Ohnishi, M. Shibata, and T. Murakami, "Motion control for advanced mechatronics," *IEEE/ASME Trans. Mechatronics*, vol. 1, no. 1, pp. 56–67, Mar. 1996.
- [36] W.-H. Chen, J. Yang, L. Guo, and S. Li, "Disturbance-observer-based control and related methods—An overview," *IEEE Trans. Ind. Electron.*, vol. 63, no. 2, pp. 1083–1095, Feb. 2016.



TAKAHARU YAMANAKA received the B.E. degree in electronics and electrical engineering from Keio University, Japan, in 2019, where he is currently pursuing the M.E. degree in integrated design engineering. He is a Student Member of the Institute of Electronics, Information and Communication Engineers (IEICE).



works.

He received the Electrical Science and Engineering Award from them the Promotion Foundation for Electrical Science and Engineering, in 2016, and the Best Paper Award from the IEEE ComSoc International Communications Quality and Reliability Workshop (CQR '17).



RYOGO KUBO (Member, IEEE) received the B.E. degree in system design engineering and the M.E. and Ph.D. degrees in integrated design engineering from Keio University, Japan, in 2005, 2007, and 2009, respectively. In 2007, he joined NTT Access Network Service Systems Laboratories, NTT Corporation, Japan. Since 2010, he has been with Keio University, where he is currently an Associate Professor with the Department of Electronics and Electrical Engineering. From 2019 to 2020, he also held the position of Honorary Research Fellow with the Department of Electronic and Electrical Engineering, University College London (UCL), U.K. His research interests include system control, optical communications, networking, and cyber-physical systems.

Dr. Kubo is a member of the Optical Society (OSA), the Institute of Electrical Engineers of Japan (IEEJ), the Institute of Electronics, Information and Communication Engineers (IEICE), and the Society of Instrument and Control Engineers (SICE). He received the Best Paper Award from the IEICE Communications Society, in 2011, the IEEE International Conference on Communications (ICC'12) Best Paper Award, in 2012, the Leonard G. Abraham Prize from the IEEE Communications Society, in 2013, and the 2018 IEEE International Conference on Intelligence and Safety for Robotics (ISR'18) Best Paper Award.

...